

Fast and reliable confidence intervals for a variance component

Yiqiao Zhang^{*} Karl Oskar Ekvall^{*,†} Aaron J. Molstad[‡]

^{*}Department of Statistics, University of Florida

[†]Division of Biostatistics, Institute of Environmental Medicine, Karolinska Institutet

[‡]School of Statistics, University of Minnesota

yiqiaozhang@ufl.edu k.ekvall@ufl.edu amolstad@umn.edu

November 5, 2024

Abstract

We show that confidence intervals in a variance component model, with asymptotically correct uniform coverage probability, can be obtained by inverting certain test-statistics based on the score for the restricted likelihood. The results apply in settings where the variance is near or at the boundary of the parameter set. Simulations indicate the proposed test-statistics are approximately pivotal and lead to confidence intervals with near-nominal coverage even in small samples. We illustrate our methods' application in spatially-resolved transcriptomics where we compute approximately 15,000 confidence intervals, used for gene ranking, in less than 4 minutes. In the settings we consider, the proposed method is between two and 28,000 times faster than popular alternatives, depending on how many confidence intervals are computed.

1 Introduction

Variance component models are widely used in applied statistics. Often, researchers are interested in quantifying how much of the variability in the data is due to a specific source, possibly after controlling for, or conditioning on, other sources of variability. It is common to assume that for non-stochastic $X \in \mathbb{R}^{n \times p}$ and $Z \in \mathbb{R}^{n \times q}$, a vector of responses $Y \in \mathbb{R}^n$ satisfies

$$Y = X\beta + ZU + E, \tag{1}$$

where $U \sim N_q(0, \sigma_g I_q)$ and, independently, $E \sim N_n(0, \sigma_e^2 I_n)$. Both U and E are unobservable, and the parameter is $\theta = (\beta, \sigma_g^2, \sigma_e^2) \in \mathbb{R}^p \times [0, \infty) \times (0, \infty)$. Equation (1) is a linear mixed model with one random effect, or several independent random effects with the same variance.

In modern genetics and genomics, the model is often written directly for the marginal distribution of Y :

$$Y \sim \mathcal{N}_n(X\beta, \sigma_g^2 K + \sigma_e^2 I_n), \quad (2)$$

where $K = ZZ^T$; see for example Purcell (2002); Kang et al. (2010); Zhang et al. (2010); Lippert et al. (2011); Yang et al. (2011); Zhou and Stephens (2012); Zhou et al. (2013); Loh et al. (2015); Weissbrod et al. (2016); Moore et al. (2019). Equations (1) and (2) give equivalent models since, for any positive semi-definite $K \in \mathbb{R}^{n \times n}$ of rank $q \leq n$, there exists a $Z \in \mathbb{R}^{n \times q}$ such that $K = ZZ^T$. In statistical genetics, when elements of Y are phenotypes for n individuals, K can be a genetic relatedness matrix quantifying similarities between individuals' common SNP genotypes (Jiang et al., 2022). Then, the quantity of inferential interest is the heritability (Visscher et al., 2008)

$$h^2 = \frac{\sigma_g^2}{\sigma_g^2 + \sigma_e^2} \in [0, 1).$$

In spatially resolved transcriptomics (Marx, 2021), when elements of Y are a gene's expression at n distinct two- or three-dimensional spatial positions in a tissue sample and K is a matrix encoding distances between positions, h^2 is known as the fraction of spatial variance (Svensson et al., 2018; Kats et al., 2021; Weber et al., 2022; Zeng et al., 2022). The parameter h^2 is related to $\tau = \sigma_g^2/\sigma_e^2$, which has been the focus of previous research on confidence intervals under (1) (e.g., Crainiceanu and Ruppert, 2004), as $h^2 = \tau/(1 + \tau)$. Because the naming of parameters is inconsistent in the literature, we refer to all of σ_g^2 , τ , and h^2 as variance components for simplicity. To be concrete, we will focus on h^2 as that is common in the motivating applications, but similar results often apply in different parameterizations. A further discussion of how our results could be extended to other parameterizations and models, including ones with more variance components or a parameterized K , is in the Supplementary Material.

Though (2) may seem a simple model, inference on h^2 can be complicated, especially when it is nearly, or equal to, zero or one, as those are boundary points of the parameter set. It is well-known that common test-statistics, such as Wald and likelihood ratio statistics, have non-standard distributions on boundary points. The distributions can often be obtained by simulation (e.g., Crainiceanu and Ruppert, 2004; Schweiger et al., 2016; Guédon et al.,

2024) or approximated, either using asymptotic theory (e.g., Self and Liang, 1987; Geyer, 1994; Stram and Lee, 1994, 1995; Baey et al., 2019), or by other means (e.g. Wood, 2013). Thus, it is often possible to construct tests with (asymptotically) correct pointwise size, and the likelihood ratio test has recently been suggested for use in related settings (Battey and McCullagh, 2023). However, creating a reliable confidence interval by inverting such a test-statistic is more complicated, for at least two reasons.

First, one in general has to compute the statistic for every relevant h^2 . Thus, methods designed specifically for testing $h^2 = 0$ are inapplicable, and simulation-based methods can be prohibitively time-consuming. Secondly, even when inverting a test with asymptotically correct pointwise size is computationally feasible, the resulting confidence region can have poor coverage properties. Specifically, the actual coverage probability often depends substantially on how close the true parameter is to the boundary. More formally, test-statistics with different asymptotic distributions on boundary and interior points lead to asymptotically *incorrect* uniform coverage probability (Ekvall and Bottai, 2022, Lemma 2.5).

To illustrate the issues, Fig. 1 shows coverage probabilities for different values of h^2 for Wald, likelihood ratio, and proposed confidence intervals defined in Section 2. For interior points of the parameter set, the confidence intervals are obtained by inverting test-statistics using quantiles of the chi-square distribution with one degree of freedom, as suggested by classical theory. Notably, the coverage probabilities for Wald and likelihood ratio intervals are substantially different from the nominal level when h^2 is near zero or one. The reason is that, when the true parameter is close to the boundary, the distributions of the test-statistics are close to what they are on the boundary. Consequently, even though the parameter is interior, classical asymptotic theory for interior points provides a poor approximation. Removing the boundary points from the parameter set or using a larger sample size is not sufficient to address the issue, as Fig. 1 illustrates; loosely speaking, for every n , there are interior points close enough to the boundary to cause problems. Asymptotic theory for related settings suggests the problematic points are within a distance of order $n^{-1/2}$ of the boundary (Rotnitzky et al., 2000; Bottai, 2003). In the Supplementary Material, we include a version of Fig. 1 with horizontal axis range $h^2 \in [.005, .01]$, where it is more clear that the problematic region indeed changes with n .

For reasons to become apparent, we focus on test-statistics based on the score and information of the restricted likelihood. By doing so we are able to construct a $(1 - \alpha)$ confidence region $\mathcal{R}_n(\alpha)$ that satisfies, for any compact subset of the parameter set, say C ,

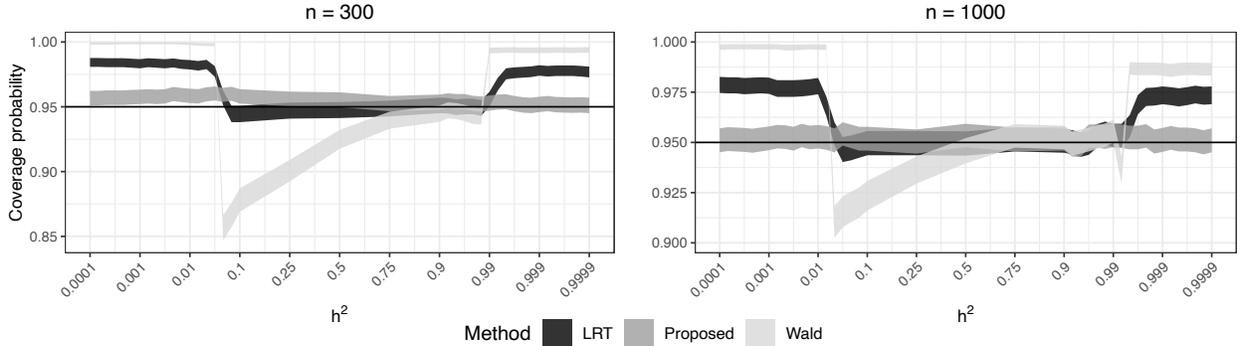


Figure 1: Monte Carlo estimates of coverage probabilities for h^2 in (2) with $\sigma_g^2 + \sigma_e^2 = 1$, $\beta = 0$, $X \in \mathbb{R}^{n \times 5}$ a matrix of independent standard normal entries, and $K_{ij} = 0.95^{|i-j|}$. The solid horizontal line indicates the nominal level. The line widths provide 95% confidence bands for the coverage probability based on 10^4 trials.

and as $n \rightarrow \infty$,

$$\sup_{\theta \in C} |\mathbb{P}_\theta\{h^2 \in \mathcal{R}_n(\alpha)\} - (1 - \alpha)| \rightarrow 0. \quad (3)$$

That is, the proposed confidence region, which is typically an interval, has asymptotically correct uniform coverage probability on compact sets. This property leads to near-nominal coverage of every practically relevant h^2 , including h^2 near or equal to zero, as is illustrated in Fig. 1. We emphasize that when focusing on uniform inference in the presence of boundary points, conclusions about score test-statistics in general do not carry over to Wald and likelihood ratio test-statistics. Indeed, our results show, in a sense to be made precise, that certain score statistics are asymptotically pivotal, but Wald and likelihood ratio test-statistics are not. The score statistics can therefore be inverted using the same quantiles for every point in the parameter set, leading to a confidence interval that is easy to implement and orders of magnitude faster to compute than competing ones. In a typical example we consider, our confidence intervals take less than a second to compute, whereas the competitors often take 500 seconds, and sometimes much longer.

Previously, the score standardized by expected information has been shown to give confidence regions with asymptotically correct uniform coverage probability in settings with singular Fisher information (Bottai, 2003; Ekvall and Bottai, 2022). We build on similar ideas here, but the setting, and hence the arguments required for the main results, are quite different. In particular, here, the information matrix is positive definite under weak conditions (Theorem 1). There are also two nuisance parameters, β and σ^2 . While dealing with β is relatively straightforward since β and (h^2, σ^2) are orthogonal in the Fisher information sense,

our results are, to the best of our knowledge, the first of their kind with non-orthogonal nuisance parameters. For instance, Ekvall and Bottai (2022) assume $\sigma_e^2 > 0$ is known. Moreover, here, the number of predictors can grow with the sample size. This is an important development as the restricted likelihood is typically used precisely when the number of predictors is smaller than the number of observations, but large enough to induce substantial bias in the inference on h^2 .

2 Model

2.1 Likelihood functions

Let $\Sigma = \text{cov}_\theta(Y) = \sigma_g^2 K + \sigma_e^2 I_n$. A log-likelihood corresponding to (2) is

$$l(\beta, \sigma_g^2, \sigma_e^2) = l(\beta, \sigma_g^2, \sigma_e^2; Y, X, K) = -\frac{1}{2} \left\{ \log |\Sigma| + (Y - X\beta)^\top \Sigma^{-1} (Y - X\beta) \right\}, \quad (4)$$

the domain of which is the parameter set $\mathbb{R}^p \times [0, \infty) \times (0, \infty)$. It is important that (4) allows $\sigma_g^2 = 0$, which is often of practical interest. When K is positive definite, points with $\sigma_e^2 = 0$ and $\sigma_g^2 > 0$ can be added to the parameter set, but with semi-definite K , (4) requires $\sigma_e^2 > 0$. Assuming X has full column rank, the restricted log-likelihood, often used for inference on the covariance parameters, is

$$l_R(\sigma_g^2, \sigma_e^2) = -\frac{1}{2} \left\{ \log |\Sigma| + \log |X^\top \Sigma^{-1} X| + (Y - X\tilde{\beta})^\top \Sigma^{-1} (Y - X\tilde{\beta}) \right\},$$

where $\tilde{\beta} = \tilde{\beta}(\sigma_g^2, \sigma_e^2) = (X^\top \Sigma^{-1} X)^{-1} X^\top \Sigma^{-1} Y$ is the partial maximizer of $l(\beta, \sigma_g^2, \sigma_e^2)$ in β , for fixed σ_g^2 and σ_e^2 . The domain of l_R is $[0, \infty) \times (0, \infty)$. The assumption that X have full column rank is for notational convenience; one could define l_R similarly as long as the column rank is less than n . Specifically, if the column rank of X is $p' < n$ and $V \in \mathbb{R}^{n \times (n-p')}$ is a semi-orthogonal matrix satisfying $V^\top X = 0$, then the restricted likelihood is the likelihood of $V^\top Y$ (Harville, 1974).

By spectral decomposition, $K = O\Lambda O^\top$ for some orthogonal $O \in \mathbb{R}^{n \times n}$ and $\Lambda = \text{diag}(\lambda_1, \dots, \lambda_n)$; here and elsewhere, eigenvalues are in decreasing order unless otherwise stated. It follows that $\Sigma = O(\sigma_g^2 \Lambda + \sigma_e^2 I_n) O^\top$ and, hence,

$$l(\beta, \sigma_g^2, \sigma_e^2) = -\frac{1}{2} \sum_{i=1}^n \left\{ \log(\lambda_i \sigma_g^2 + \sigma_e^2) + \frac{(O^\top Y - O^\top X\beta)_i^2}{\lambda_i \sigma_g^2 + \sigma_e^2} \right\},$$

where $(\cdot)_i$ means the i th element; and

$$l_R(\sigma_g^2, \sigma_e^2) = l(\tilde{\beta}, \sigma_g^2, \sigma_e^2) - \log |(O^T X)^T (\sigma_g^2 \Lambda + \sigma_e^2 I_n)^{-1} O^T X|/2.$$

Thus, when developing theory, we may upon replacing Y and X by $O^T Y$ and $O^T X$, respectively, assume diagonal covariance matrices $K = \Lambda$ (equivalently, $O = I_n$) and $\Sigma = \sigma_g^2 \Lambda + \sigma_e^2 I_n$ without loss of generality. When doing so, the observations are ordered so that the i th response Y_i corresponds to the i th eigenvalue λ_i .

At the expense of more notation, the assumption on Σ could be relaxed to $\Sigma = \sigma_g^2 K + \sigma_e^2 W$ for some known positive definite $W \in \mathbb{R}^{n \times n}$. Indeed, in that case Y , X , and K can be replaced by, respectively, $W^{-1/2} Y$, $W^{-1/2} X$, and $W^{-1/2} K W^{-1/2}$ before repeating the above argument to get a diagonal Σ .

In several motivating applications, the parameter of interest is $h^2 = \sigma_g^2 / (\sigma_g^2 + \sigma_e^2)$. Therefore, we consider a common reparameterization in terms of h^2 and $\sigma^2 = \sigma_g^2 + \sigma_e^2$. Then, $\Sigma = \sigma^2 O \{h^2 \Lambda + (1 - h^2) I_n\} O^T$. Overloading the letter l and assuming $O = I_n$ without loss of generality, the log-likelihood becomes

$$l(\beta, h^2, \sigma^2) = -\frac{1}{2} \sum_{i=1}^n \left\{ \log(\sigma^2) + \log(\lambda_i h^2 + 1 - h^2) + \frac{(Y_i - X_i^T \beta)^2}{\sigma^2 (\lambda_i h^2 + 1 - h^2)} \right\}, \quad (5)$$

where X_i^T is the i th row of X . The domain of l is the parameter set $\mathbb{R}^p \times [0, 1) \times (0, \infty)$. The corresponding restricted log-likelihood, with domain $[0, 1) \times (0, \infty)$, is

$$l_R(h^2, \sigma^2) = l(\tilde{\beta}, h^2, \sigma^2) + \frac{p}{2} \log(\sigma^2) - \frac{1}{2} \log |X^T \{h^2 \Lambda + (1 - h^2) I_n\}^{-1} X|.$$

2.2 Test-statistics and confidence regions

There are many potential test-statistics for inference based on $l(\beta, h^2, \sigma^2)$ and $l_R(h^2, \sigma^2)$. However, most common ones, like Wald and likelihood ratio statistics, do not give confidence regions satisfying (3) in boundary settings in general. Therefore, we focus on score statistics standardized to have mean zero and diagonal covariance matrix. Such test-statistics have previously been shown to lead to results like (3) in settings where, unlike here, the Fisher information is singular (Ekvall and Bottai, 2022). Because our goal is to construct confidence regions for the covariance parameters, effectively treating β as a nuisance parameter, we primarily work with the restricted likelihood.

Let $V_1 = V_1(h^2, \sigma^2) = \partial \Sigma / \partial h^2 = \sigma^2 O (\Lambda - I_n) O^T$ and $V_2 = V_2(h^2, \sigma^2) = \partial \Sigma / \partial \sigma^2 = O (h^2 \Lambda +$

$(1 - h^2)I_n)O^\top$. Similarly, let $U_1(h^2, \sigma^2) = \partial l_R(h^2, \sigma^2)/\partial h^2$ and $U_2(h^2, \sigma^2) = \partial l_R(h^2, \sigma^2)/\partial \sigma^2$, so the restricted score is $U(h^2, \sigma^2) = [U_1(h^2, \sigma^2), U_2(h^2, \sigma^2)]^\top$. Routine calculations show, for $j \in \{1, 2\}$,

$$U_j(h^2, \sigma^2) = \frac{1}{2}(Y - X\tilde{\beta})^\top \Sigma^{-1} V_j \Sigma^{-1} (Y - X\tilde{\beta}) - \frac{1}{2} \text{tr}(\Sigma^{-1} V_j) + \frac{1}{2} \text{tr}(\Sigma^{-1} X (X^\top \Sigma^{-1} X)^{-1} X^\top \Sigma^{-1} V_j).$$

Observe U_j is defined on $[0, 1) \times (0, \infty)$ and has a continuous extension to points where $h^2 = 1, \sigma^2 > 0$ if K is positive definite. The expression simplifies substantially for $j = 2$ since $V_2 = \Sigma/\sigma^2$. Specifically, assuming $O = I_n$,

$$U_2(h^2, \sigma^2) = -\frac{n-p}{2\sigma^2} + \frac{1}{2\sigma^4} \sum_{i=1}^n \frac{(Y_i - X_i^\top \tilde{\beta})^2}{h^2 \lambda_i + 1 - h^2}. \quad (6)$$

Let $\mathcal{I}(h^2, \sigma^2)$ denote the restricted information matrix, that is, the covariance matrix of $U(h^2, \sigma^2)$ when h^2 and σ^2 are the true parameters. We next give an expression for $\mathcal{I}(h^2, \sigma^2)$ for easy reference. The proof, along with those of other formally stated results, is in the Supplementary Material.

Let $P = \Sigma^{-1/2} X (X^\top \Sigma^{-1} X)^{-1} X^\top \Sigma^{-1/2}$, $Q = I_n - P$, $D = \{h^2 \Lambda + (1 - h^2)I_n\}^{-1} (\Lambda - I_n)$, and $H = ODO^\top$.

Proposition 1. *If (2) holds for some X with full column rank, then the restricted information matrix has elements*

$$\mathcal{I}_{11}(h^2, \sigma^2) = \frac{1}{2} \text{tr}(QHQH); \quad \mathcal{I}_{12}(h^2, \sigma^2) = \frac{1}{2\sigma^2} \text{tr}(QH); \quad \mathcal{I}_{22}(h^2, \sigma^2) = \frac{n-p}{2\sigma^4}.$$

For inference on (h^2, σ^2) jointly, we consider the (quadratic) restricted score standardized by the restricted information:

$$T_n^R(h^2, \sigma^2) = U(h^2, \sigma^2)^\top \mathcal{I}^{-1}(h^2, \sigma^2) U(h^2, \sigma^2), \quad (7)$$

For inference on h^2 only, we use

$$T_n^R(h^2) = U_1(h^2, \tilde{\sigma}^2)^2 \mathcal{I}^{11}(h^2, \tilde{\sigma}^2), \quad (8)$$

where $\mathcal{I}^{11}(h^2, \sigma^2)$ is the leading element of $\mathcal{I}^{-1}(h^2, \sigma^2)$ and $\tilde{\sigma}^2 = \tilde{\sigma}^2(h^2)$ is the partial maximizer

of $l_R(h^2, \sigma^2)$ in σ^2 , for a fixed h^2 . By (6), assuming $O = I_n$,

$$\tilde{\sigma}^2 = \frac{1}{n-p} \sum_{i=1}^n \frac{(Y_i - X_i^T \tilde{\beta})^2}{h^2 \lambda_i + 1 - h^2} = \frac{1}{n-p} (Y - X \tilde{\beta})^T \{h^2 \Lambda + (1 - h^2) I_n\}^{-1} (Y - X \tilde{\beta}). \quad (9)$$

When X has column rank less than n , $\tilde{\sigma}^2$ is greater than zero with probability one, and hence a valid partial maximizer. Note $\tilde{\beta}$ does not depend on σ^2 , so the last display indeed gives an explicit expression for $\tilde{\sigma}^2$. For inference on h^2 , we sometimes also consider $S_n^R(h) = U_1(h^2, \tilde{\sigma}^2) \mathcal{I}^{11}(h^2, \tilde{\sigma}^2)^{1/2}$, that is, the signed square root of (8).

The proposed test-statistics require a positive definite $\mathcal{I}(h^2, \sigma^2)$, which the following result establishes. Notably, $\mathcal{I}^{11}(h^2, \sigma^2)$ is positive if $\mathcal{I}(h^2, \sigma^2)$ is positive definite. To understand the next result, notice that Q has rank $n - p$, so QHQ has at most $n - p$ non-zero eigenvalues, and recall $V \in \mathbb{R}^{n \times (n-p)}$ is a semi-orthogonal matrix such that $V^T X = 0$.

Theorem 1. *The information matrix $\mathcal{I}(h^2, \sigma^2)$ is singular if and only if the following equivalent conditions hold: (i) the $n - p$ possibly non-zero eigenvalues of QHQ are identical; (ii) $V^T K V = c I_{n-p}$ for some $c \geq 0$.*

The proof of Theorem 1 is relatively straightforward using the expressions in Proposition 1. The key observation is that the determinant of $\mathcal{I}(h^2, \sigma^2)$ is

$$\frac{1}{2\sigma^4} \left\{ (n-p) \operatorname{tr}(QHQQHQ) - \operatorname{tr}(QHQ)^2 \right\},$$

which is strictly positive by Jensen's inequality applied to the $n - p$ possibly non-zero eigenvalues of QHQ unless they are all identical, in which case the determinant is zero.

Theorem 1 is particularly intuitive if $p = 0$, so that $Q = V = I_n$. Then the eigenvalues of QHQ are the diagonal elements of D , which are identical if and only if the diagonal elements of Λ are; that is, if and only if Λ , and hence K , is proportional to the identity. The parameters are unidentifiable for such K , so we will generally assume K is not proportional to the identity, leading to a positive definite information matrix.

By inverting the proposed test-statistics using quantiles from chi-squared distributions, we get the confidence regions

$$\begin{aligned} \mathcal{R}_n(\alpha) &= \{h^2 \in [0, 1] : T_n^R(h^2) \leq q_{1-\alpha, 1}\}; \\ \mathcal{R}_n^2(\alpha) &= \{(h^2, \sigma^2) \in [0, 1] \times (0, \infty) : T_n^R(h^2, \sigma^2) \leq q_{1-\alpha, 2}\}. \end{aligned} \quad (10)$$

When $h^2 = 1$ is not in the parameter set, we take $T_n^R(1) = T_n^R(1, \sigma^2) = \infty$ so the confidence

regions are well defined.

3 Asymptotic distributions

We assume $K_n = \Lambda_n = \text{diag}(\lambda_{n1}, \dots, \lambda_{nn})$ in this section without loss of generality, and hence $\Sigma_n = \sigma_n^2\{(1 - h_n)I_n + h_n\Lambda_n\}$ and $H_n = D_n$ are diagonal. Here, a subscript n has been added to σ^2 and other quantities since we will consider a sequence $\{(\beta_n, h_n^2, \sigma_n^2)\}$ of parameters indexed by the sample size, and a corresponding sequence of models. Similarly, the number of predictors $p = p_n$ can change with n . By considering a sequence of (true) parameters, we can obtain the asymptotic distribution of $T_n^R(h_n^2, \sigma_n^2)$ and $T_n^R(h_n^2)$ under that sequence. This is useful because (3) holds for $\mathcal{R}_n(\alpha)$ in (10) if and only if the asymptotic distribution of $T_n^R(h_n^2)$ is the same under any convergent sequence of parameters (Ekvall and Bottai, 2022, Lemma 2.5), and similarly for $\mathcal{R}_n^2(\alpha)$. This result essentially follows from the equivalence of continuous convergence and uniform convergence on compact sets, applied to the sequence of functions defined by $\theta \mapsto \text{P}_\theta\{T_n^R(h^2) \leq q_{1-\alpha,1}\}$. More generally, examining the distribution under a sequence of parameters tending to a point, can lead to a better understanding of the behavior of the test-statistic near that point. Thus, for our purposes, sequences tending to boundary points are of particular interest. The next result is our first along these lines.

To state the result, let $\gamma_i(\cdot)$ denote the i th eigenvalue in decreasing order.

Lemma 1. *Assume that, for every $n \in \{1, 2, \dots\}$, Y satisfies (2) with an X with full column rank, $K_n = \Lambda_n$, and parameters $(\beta_n, h_n^2, \sigma_n^2)$. If, as $n \rightarrow \infty$, (i) $p/n \rightarrow 0$, (ii) $\sum_{i=1}^p \gamma_i(D_n^2)/\text{tr}(D_n^2) \rightarrow 0$, (iii) $\limsup_{n \rightarrow \infty} \{n^{-1} \text{tr}(D_n)^2/\text{tr}(D_n^2)\} < 1$; then, in distribution,*

$$T_n^R(h_n^2, \sigma_n^2) \rightarrow \chi_2^2. \quad (11)$$

The proof of Lemma 1 establishes (11) by showing asymptotic bivariate normality of $\mathcal{I}_n(h_n^2, \sigma_n^2)^{-1/2}U_n(h_n^2, \sigma_n^2)$. The key observation is that the elements of $U_n(h_n^2, \sigma_n^2)$ are quadratic forms in multivariate normal vectors, centered to have mean zero. Therefore, their distributions are those of linear combinations of independent chi-square random variables. The conditions of the theorem ensure Lyapunov's central limit theorem applies to those linear combinations.

Conditions (ii) and (iii) concern Λ_n and h_n^2 , but neither of β_n and σ_n^2 appears in the conditions. Thus, (11) can hold for sequences one may not expect, such as those where $\sigma_n^2 \rightarrow 0$. This suggests the behavior of our test-statistic is insensitive to the true σ^2 , and may

perform well even if σ^2 is near the boundary, that is, near zero.

Condition (ii) says the sum of the p greatest eigenvalues of D_n^2 should be negligible compared to the sum of all its eigenvalues. An eigenvalue, or diagonal element, of D_n^2 will be relatively large if either (a) the corresponding element of Λ_n is relatively close to zero and h^2 is close to one, or (b) the corresponding element of Λ_n is relatively large. Thus, condition (ii) suggests the test-statistic may not behave well if a few elements of $O^T Y$ have much larger variance than all other ones, or if some elements have very small variance and most of it is attributable to K .

Condition (iii) essentially says that, when comparing the squared average of the eigenvalues of D_n to the average of the squared eigenvalues, Jensen's inequality is asymptotically strict; there has to be non-negligible variation in the diagonal elements of D_n . This is intuitive as, if all the diagonal elements of D_n are the same, then Λ_n is proportional to the identity and h_n^2 unidentifiable, as noted in the remark following Theorem 1.

Conditions (ii) and (iii) could be replaced by slightly weaker ones by adding assumptions on how X relates to K , but that would substantially increase notational burden.

Our next result shows that the proposed test-statistic for h^2 has the desired asymptotic distribution under the conditions of Lemma 1. Substantial work is needed to establish the result since σ^2 is a nuisance parameter for the purposes of inference on h^2 only. In particular, the test-statistic for h^2 cannot depend on or be evaluated at the true parameter, or null hypothesis, which was possible in Lemma 1.

Lemma 2. *Under the conditions of Lemma 1, $T_n^R(h_n^2) \rightarrow \chi_1^2$ in distribution as $n \rightarrow \infty$.*

Lemma 2 is proven by showing that $T_n(h_n^2)$ has the same asymptotic distribution as $\{U_{n1} - \mathcal{I}_{n12}U_{n2}/\mathcal{I}_{n22}\}^2 \mathcal{I}_n^{(11)}$, with all quantities evaluated at the true (h_n^2, σ_n^2) and $\mathcal{I}_n^{(11)}$ denoting the leading element of \mathcal{I}_n^{-1} . This result is consistent with what is often obtained for nuisance parameters in classical settings, with fixed interior parameters (Cox and Hinkley, 2000, Section 9.3). This is remarkable because those results in general do not apply under sequences of parameters or with boundary points.

Our next result gives intuitive conditions on model parameters and K which ensure the conditions in Lemmas 1 and 2 hold. The conditions are not necessary in general, but they are more transparent, and easier to assess in practice, than those in the lemmas.

Theorem 2. *Assume that, for every $n \in \{1, 2, \dots\}$, Y satisfies (2) with an X with full column rank and parameters $(\beta_n, h_n^2, \sigma_n^2)$. If (i) $\lim_{n \rightarrow \infty} p_n/n = 0$; (ii*) $\limsup_{n \rightarrow \infty} \lambda_{n1} < \infty$; (iii*) $\liminf_{n \rightarrow \infty} \lambda_{nn} > 0$ or $\limsup_{n \rightarrow \infty} h_n^2 < 1$; (iv*) there exists an $\epsilon > 0$ such that for any*

$c \in [0, \infty)$, with k_n^c denoting the number of eigenvalues of Λ_n in $[c - \epsilon, c + \epsilon]$, it holds that $\limsup_{n \rightarrow \infty} k_n^c/n < 1$, then, in distribution as $n \rightarrow \infty$,

$$T_n^R(h_n^2, \sigma_n^2) \rightarrow \chi_2^2; \quad T_n^R(h_n^2) \rightarrow \chi_1^2. \quad (12)$$

Since Λ_n is known, condition (ii*) can be made to hold, for example by replacing K by K/λ_{n1} . Then, for the conclusions to hold, conditions (iii*) and (iv*) would need to hold for the new eigenvalues $\lambda_{ni}/\lambda_{n1}$, $i \in \{1, \dots, n\}$. Condition (iii*) illustrates that if K is full rank, then reliable inference on h^2 near one is possible; this is formalized further in Corollary 1. Condition (iv*) prevents the eigenvalues of K from concentrating in some neighborhood asymptotically. That is, it prevents K from being essentially proportional to the identity asymptotically.

Corollary 1. *Under condition (i), (ii*), and (iv*) of Theorem 2, $\mathcal{R}_n(\alpha)$ and $\mathcal{R}_n^2(\alpha)$ in (10) have asymptotically correct uniform coverage probability on compact subsets of $[0, 1)$ and $[0, 1) \times (0, \infty)$, respectively (c.f. (3)). The conclusion can be strengthened to compact subsets of $[0, 1] \times (0, \infty)$ and $[0, 1]$, respectively, if the first part of condition (iii*) of Theorem 2 also holds.*

4 Computational considerations

In this section, we consider the computational aspects of our test-statistics. Like popular competing methods, we require a one-time preprocessing step where the eigendecomposition of $K = O\Lambda O^T$ is used to construct $Y_O = O^T Y$ and $X_O = O^T X$. In some applications, the same K is used for many different choices of response vector Y , with separate inference on h^2 for each response vector. Then, the pre-processing step is only performed once.

We show that, after the pre-processing, the number of floating point operations required to evaluate the proposed test-statistics grows linearly in n , making our methods feasible for large-scale applications, such as those described in Section 1. More specifically, we show that, if p is potentially growing with n , the number of operations required is $O(np^2 + p^3)$.

Recall $V_2 = h^2\Lambda + (1-h^2)I_n$ and define $\tilde{P} = V_2^{-1/2} X_O (X_O^T V_2^{-1} X_O)^{-1} X_O^T V_2^{-1/2}$, $\tilde{Q} = I_n - \tilde{P}$, $\tilde{\beta} = (X_O^T V_2^{-1} X_O)^{-1} X_O^T V_2^{-1} Y_O$, and $\tilde{R} = Y_O - X_O \tilde{\beta}$. Let \tilde{R}_i denote the i th element of \tilde{R} and

Q_{ii} the i th diagonal element of Q . The score function is then

$$U(h^2, \sigma^2) = \frac{1}{2} \begin{pmatrix} \sum_{i=1}^n D_{ii} \left(\frac{\sigma^{-2} \tilde{R}_i^2}{h^2 \lambda_i + 1 - h^2} - \tilde{Q}_{ii} \right) \\ -\frac{n-p}{\sigma^2} + \frac{1}{\sigma^4} \sum_{i=1}^n \frac{\tilde{R}_i^2}{h^2 \lambda_i + 1 - h^2} \end{pmatrix}. \quad (13)$$

Both terms in (13) involve the summation of n terms. Construction of \tilde{R} requires $O(np)$ operations, and computation of all \tilde{Q}_{ii} requires $O(np^2)$ operations. We do not compute or store the entire matrix \tilde{Q} .

To compute the information efficiently, note $Q = O\tilde{Q}O^T$, so by Proposition 1,

$$\mathcal{I}(h^2, \sigma^2) = \frac{1}{2\sigma^4} \begin{pmatrix} \sigma^4 \text{tr}(\tilde{Q}D\tilde{Q}D) & \sigma^2 \text{tr}(\tilde{Q}D) \\ \sigma^2 \text{tr}(\tilde{Q}D) & n-p \end{pmatrix}.$$

Because $\text{tr}(\tilde{Q}D) = \sum_{i=1}^n \tilde{Q}_{ii}D_{ii}$, \mathcal{I}_{12} can be evaluated in $O(n)$ operations using the \tilde{Q}_{ii} computed before. Notice $2\mathcal{I}_{11} = \text{tr}(\tilde{Q}D\tilde{Q}D) = \text{tr}(D^2) - 2\text{tr}(\tilde{P}D^2) + \text{tr}(\tilde{P}D\tilde{P}D)$. Because D is a diagonal matrix, evaluating $\text{tr}(D^2)$ requires $O(n)$ operations. Similarly, $\text{tr}(\tilde{P}D^2) = \sum_{i=1}^n (1 - \tilde{Q}_{ii})D_{ii}^2$, so evaluating this term also requires only $O(n)$ operations. Finally, by the cyclic property of the trace operator, $\text{tr}(\tilde{P}D\tilde{P}D) = \text{tr}(\tilde{A}\tilde{B}\tilde{A}\tilde{B})$ where $\tilde{A} = (X_O^T V_2^{-1} X_O)^{-1} \in \mathbb{R}^{p \times p}$ and $\tilde{B} = X_O^T V_2^{-1/2} D V_2^{-1/2} X_O \in \mathbb{R}^{p \times p}$. Thus, evaluating $\text{tr}(\tilde{A}\tilde{B}\tilde{A}\tilde{B})$ requires $O(np^2 + p^3)$ operations, with the p^3 coming from a Cholesky (or other) decomposition of \tilde{A}^{-1} to deal with the inverse, and the np^2 is from matrix multiplications.

We have created an R package `lmmvar` for computing our test-statistics and confidence intervals, available for download at github.com/yqzhang5972/lmmvar. The package also provides an implementation of the method by Crainiceanu and Ruppert (2004).

A confidence interval for h^2 can be obtained by evaluating $T_n^R(h^2)$ from at equally spaced points in $[0, 1)$ and comparing the values to quantiles from the chi-square distribution with one degree of freedom. In practice, however, it is typically possible, and faster, to do a search for the points where $T_n^R(h^2)$ crosses the desired quantile. More specifically, when $T_n^R(h^2)$ is strictly quasiconvex in h^2 , then $\mathcal{R}_n(\alpha)$ is an interval, so we need only search for points a such that $T_n^R(a) = q_{1,1-\alpha}$. While we have not been able to prove $T_n^R(h^2)$ is quasiconvex in general due to technical difficulties, we have not encountered an example where it is not. Typically, $T_n^R(h^2)$ looks roughly like one of the three cases in Fig. 2. Thus, in our software we first find a point a' such that $T_n^R(a') < q_{1,1-\alpha}$. More specifically, we start a ternary search for the minimum of T_n^R and terminate the first time a value less than $q_{1,1-\alpha}$ is encountered. Then, under quasiconvexity and assuming a' is not on the boundary, the intervals $[0, T_n^R(a')]$ and

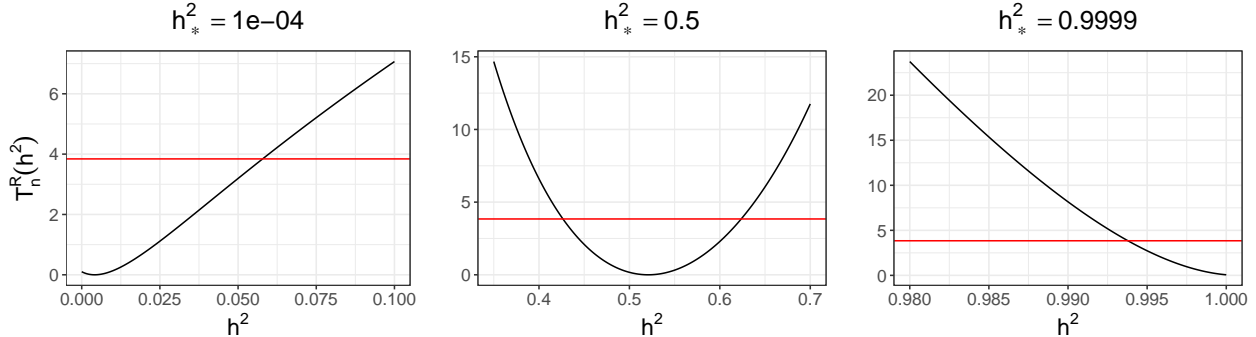


Figure 2: The value $T_n^R(h^2)$ with $n = 1000$, data generated under the same model as in Fig. 1, and the true h^2 , here denoted h_*^2 , taking values 0.0001, 0.5, and 0.999. Horizontal red lines indicate the 95th percentile of the χ_1^2 distribution.

$[T_n^R(a'), 1)$ contain lower and upper bounds of the interval $\mathcal{R}_n(\alpha)$, respectively. We then use a bisection search to find $b \in [0, T_n^R(a')]$ such that $T_n^R(b) = q_{1,1-\alpha}$, and similarly for $[T_n^R(a'), 1)$. If the point a' is on the boundary, as in the first and third plot of Fig. 2, only one bisection search is needed. In either case, this procedure often requires less computing time than a grid search.

We have also found that, in practice, $S_n^R(h^2) = \{\mathcal{I}_n^{11}(h^2, \tilde{\sigma}^2)\}^{1/2} U_1(h^2, \tilde{\sigma}^2)$ is typically monotonely decreasing in h^2 , so a search can also be based on that statistic and comparisons to standard normal quantiles; see Section 5.3 for an example with one-sided confidence intervals.

5 Numerical studies

5.1 Finite-sample interval width and coverage probabilities

To supplement our asymptotic theory, we study how n , h^2 , and the eigenvalues of K affect the coverage probability and width of our confidence intervals. We consider $K_{ij} = \rho^{|i-j|}$ for $\rho \in (0, 1)$ and $i, j \in \{1, \dots, n\}$. When ρ is close to one, K is approximately $1_n 1_n^T$, where 1_n is an n -vector of ones. Thus, approximately, $\lambda_{n1} = n$ and $\lambda_{ni} = 0$, $i \geq 2$, which is inconsistent with conditions (ii*) and (iv*) of Theorem 2. Conversely, when ρ is close to zero, K is approximately an identity matrix, which is inconsistent with condition (iv*) of Theorem 2. Thus, we expect our test-statistic to perform best when ρ is not too close to either zero or one.

In each setting considered, we generate $X \in \mathbb{R}^{n \times 5}$ with independent and identically

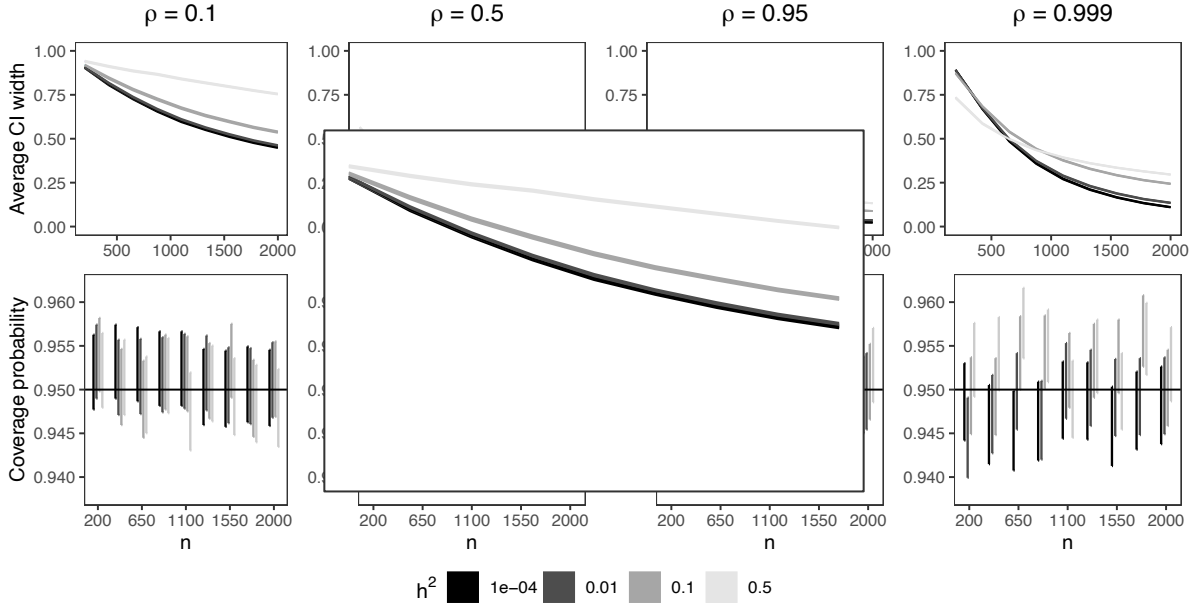


Figure 3: (Top panel) The average width of our confidence interval for h^2 and (bottom panel) the average coverage probability as n varies with $\rho \in \{0.1, 0.5, 0.95, 0.999\}$. In the top panels, the widths of the lines provide 95% confidence bands; and in the bottom panel, the bars contain the 95% confidence intervals, each based on 10^4 trials.

distributed standard normal entries, and then generate $Y \sim \mathcal{N}_n(X\beta, h^2K + (1 - h^2)I_n)$ (i.e., $\sigma^2 = 1$) with $\beta = 0$. For every combination of the triplet (n, h^2, ρ) , we generate 10^4 independent realizations of Y and compute the corresponding 95% confidence intervals for h^2 for each realization. Thus, coverage probability and average width intervals in Figure. 3 are estimated based on 10^4 independent replicates.

The bottom panel of Fig. 3 displays coverage probabilities with ρ and n varying for four different values of h^2 . For $\rho \in \{0.1, 0.5, 0.95\}$, our interval appears to have the coverage probability 0.95 or higher. Only when $\rho = 0.999$ is the evidence of under-coverage for some combinations of n and h^2 .

The top panel of Fig. 3 displays interval widths for different values of ρ and h^2 . When $\rho = 0.1$, $K \approx I_n$, which means h^2 is approximately unidentifiable. Consequently, interval widths are too large to be practically useful, despite having the nominal coverage level. With $\rho = 0.5$ or 0.95, the widths are reasonably small and decrease as n increases. When $\rho = 0.999$, the eigenvalues of K are approximately $(n, 0, \dots, 0)$, which appear to lead to longer confidence intervals. Nevertheless, as n increases, interval widths decrease as expected. As n approaches 2000, the widths are small enough to be useful in practice.

5.2 Comparison to simulation-based test-statistics

Existing methods for constructing confidence intervals for h^2 often rely on simulation. For example, Schweiger et al. (2016) uses the parametric bootstrap to approximate the distribution of the restricted maximum likelihood estimator of h^2 . In comparison to a naive implementation of the parametric bootstrap, their implementation is very efficient. Specifically, to estimate the distribution of the estimator when the true heritability is h^2 , their method requires (i) drawing N independent samples from (2) with $\sigma^2 = 1$ and null hypothesis value h^2 given; and (ii) for each sample, finding an interval containing a local maximizer of the restricted log-likelihood. Since each sample is needed for step (ii), Schweiger et al. (2016) show that it is sufficient to draw samples from $\mathcal{N}_n(0, I_n)$ in step (i) and modify step (ii) accordingly. The modified step (ii) is performed by evaluating the derivative of the restricted log-likelihood at fixed grid points. However, for a given h^2 the derivative must, in general, be evaluated at many grid points; and this procedure must be repeated for all N samples. Constructing confidence intervals thus requires repeating this procedure many times, which can be computationally burdensome. Nevertheless, the procedure is faster than previous state-of-the-art simulation-based method due to Crainiceanu and Ruppert (2004). The latter method provides an interval for $\tau = \sigma_g^2/\sigma_e^2$, which is straightforward to turn into an interval for $h^2 = \tau/(1 + \tau)$.

In follow-up work, Schweiger et al. (2018) proposed a stochastic approximation to the confidence intervals of Schweiger et al. (2016). The approximation estimates the upper and lower bounds of the confidence interval using the Robbins–Monro algorithm. Like our test-statistic, after the same preprocessing step, the number of operations required for constructing their intervals scales linearly with n .

In Fig. 4, we compare the time needed to compute our interval to those of Schweiger et al. (ALBI, 2016), Schweiger et al. (FIESTA, 2018) and Crainiceanu and Ruppert (RLRT, 2004). The figure indicates our confidence intervals can be computed most efficiently. For example, when $n = 200$ and $h^2 = 0.01$ our method took on average 7.3×10^{-4} seconds compared to 2.89 seconds, 69.98 seconds and 327.10 for FIESTA, ALBI and RLRT, respectively. When $n = 2000$ and $h^2 = 0.01$, our method took 0.02 seconds on average, whereas FIESTA, ALBI and RLRT took 119.38 seconds, 736.51 seconds and 3983.35 seconds respectively. ALBI and FIESTA are written in Python, while our software and RLRT are written in R and C++. All timings were obtained simultaneously on the University of Florida’s high-performance computing cluster, HiPerGator.

We also compared the widths of our confidence intervals to those of Schweiger et al. (2016).

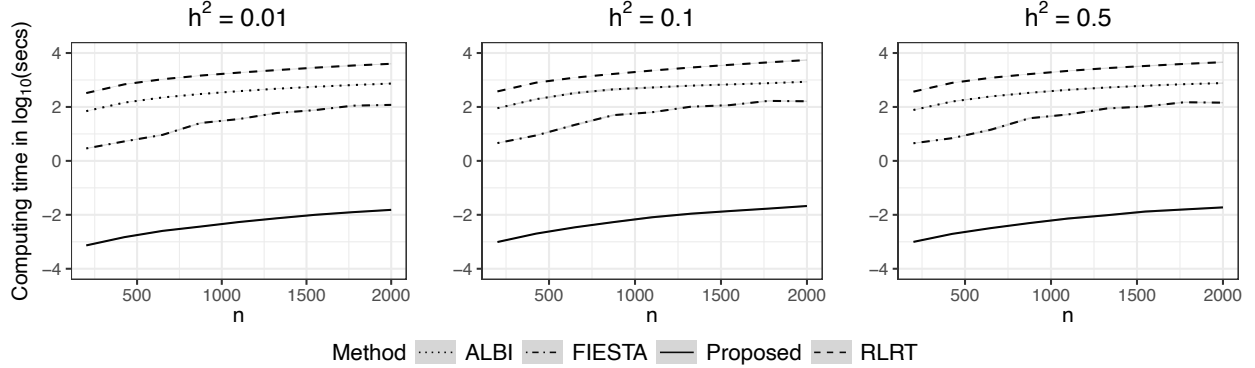


Figure 4: Average computing times for one confidence interval for h^2 using the methods proposed here (“Proposed”), by Schweiger et al. (2016) (“ALBI”), by Schweiger et al. (2018) (“FIESTA”), and by Crainiceanu and Ruppert (2004) (“RLRT”). There are shaded regions providing 95% confidence bands. All times exclude the required eigendecomposition of K . Data were generated under the same model as in Fig. 1.

We found that under a broad range of settings, the distribution of the widths were similar. In the Supplementary Material, we provide plots comparing the two intervals’ widths for $n \in \{200, 500, 1000, 2000\}$ and h^2 varying. Due to the long computing times for the interval of Crainiceanu and Ruppert (2004), we excluded it from these comparisons.

5.3 Gene ranking in spatially-resolved transcriptomics

In Section 1, we described one application of our method in the analysis of spatially resolved transcriptomic data. The rightmost panels of Fig. 5 display data generated in a spatially resolved RNA sequencing experiment performed on a mouse brain tissue sample. In such an experiment, one measures the expression of thousands of genes (the number of RNA reads aligning with each gene) from cells in 50 micron diameter spatial locations (known as spots) across the tissue sample slice. These spots are represented by the colored circles in the rightmost panels of Fig. 5; expression is measured separately in each spot.

In this context, for one gene, h^2 is the fraction of variability in expression attributed to the spatial orientation of the tissue sample. In a typical analysis, one tests h^2 for more than 10,000 genes. Specifically, it is common to assume that for the ℓ th gene, the vector of normalized random expression in all spots Y_ℓ , satisfies

$$Y_\ell \sim \mathcal{N}_n(X\beta_\ell, \sigma_\ell^2\{h_\ell^2 K + (1 - h_\ell^2)I_n\}), \quad \ell \in \{1, \dots, d\}, \quad (14)$$

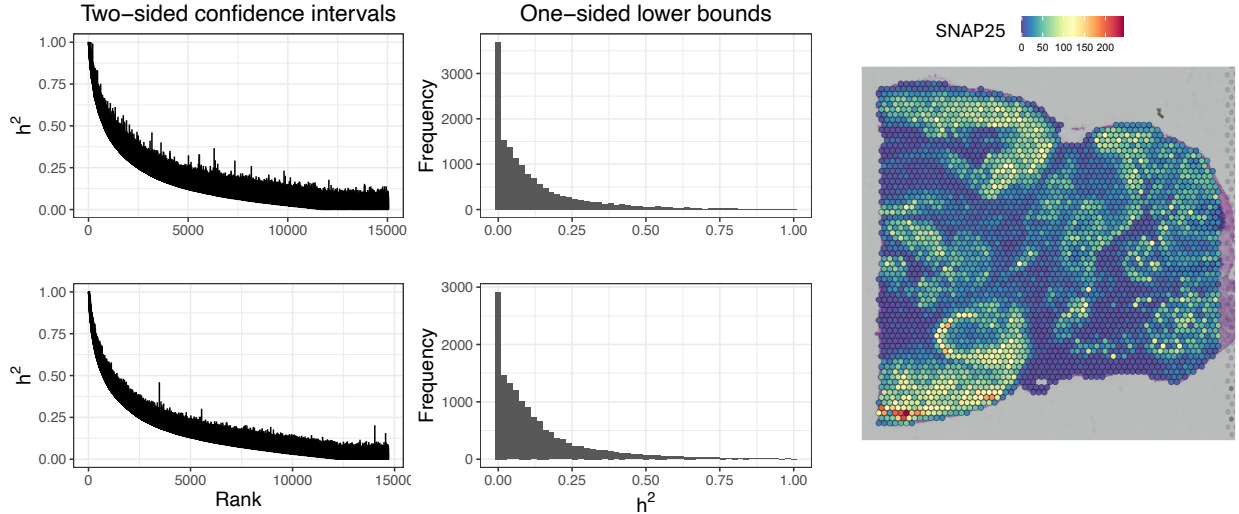


Figure 5: (Left panels) Two-sided 95% confidence intervals for h^2 in anterior (top row) and posterior (bottom row) regions of a mouse’s brain tissue, sorted according to their lower bound. (Middle panels) Histograms of the lower bounds of 95% one-sided confidence intervals for h^2 in both anterior and posterior regions. (Right panel) Expression counts of SNAP25, one of the most spatially variable genes, across the posterior region. We display counts, but our analysis is performed on log-normalized expression.

where h_ℓ^2 is the fraction of spatial variability in the ℓ th gene, n is the number of spots in the tissue, d is the number of genes in the study, and Y_ℓ and $Y_{\ell'}$ are independent for all $\ell \neq \ell'$. Typically $K_{ij} = \exp(-\|s_i - s_j\|/a)$ for some fixed $a > 0$, where s_i is the two-dimensional spatial coordinates of the i th spot and $\|\cdot\|$ is the Euclidean norm.

To demonstrate the usefulness of our method in this application, we analyzed two separate slices of a mouse’s brain tissue (anterior and posterior regions), which are available as the *stxbrain* data in the `SeuratData` R package. These data were generated on the 10X Visium platform. Assuming (14) with $a = 0.02$ (chosen based on results from Weber et al. (2022)), after quality control of filtering out low-expressed genes and boundary spots in the tissues, $n = 2380$ for $d = 15117$ genes in the anterior slice and $n = 3011$ for $d = 14738$ genes in the posterior slice.

Using our test statistics, we can provide a confidence interval for each h_ℓ^2 . Moreover, in order to rank genes, we can also provide one-sided confidence intervals for h_ℓ^2 by comparing $U_1(h^2, \tilde{\sigma}^2)\{\mathcal{I}^{11}(h^2, \tilde{\sigma}^2)\}^{1/2}$ to quantiles of the standard normal distribution.

Because K does not depend on ℓ , we can perform a transcriptome-wide analysis very efficiently. After a one-time eigendecomposition of K , the remaining processes took around 3 minutes and 4 minutes for the two tissue regions, respectively. For comparison, ALBI took

approximately 9 minutes and 13 minutes for the two tissues, including the time needed to find the necessary maximum likelihood estimates of each h_{ℓ}^2 , which was around 3 minutes. FIESTA, which is generally slower than ALBI when computing many confidence intervals, timed out after 96 hours.

Acknowledgement

The authors thank an Associate Editor and two anonymous referees for comments leading to a substantially improved manuscript. The authors also thank Yu-Ru Su for a helpful conversation, and Regev Schweiger for assistance with ALBI, FIESTA, and for providing useful references. A. J. Molstad's research was supported in part by a grant from the National Science Foundation (DMS-2413294).

Supplementary material

Proofs of lemmas and theorems are in the Supplementary Material.

References

- Baey, C., Cournède, P.-H., and Kuhn, E. (2019). Asymptotic distribution of likelihood ratio test statistics for variance components in nonlinear mixed effects models. *Computational Statistics & Data Analysis*, 135:107–122.
- Bathey, H. S. and McCullagh, P. (2023). An anomaly arising in the analysis of processes with more than one source of variability. *Biometrika*, page asad044.
- Bottai, M. (2003). Confidence regions when the Fisher information is zero. *Biometrika*, 90(1):73–84.
- Cox, D. R. and Hinkley, D. V. (2000). *Theoretical Statistics*. Chapman & Hall/CRC, Boca Raton.
- Crainiceanu, C. M. and Ruppert, D. (2004). Likelihood ratio tests in linear mixed models with one variance component. *Journal of the Royal Statistical Society: Series B (Statistical Methodology)*, 66(1):165–185.

- Ekvall, K. O. and Bottai, M. (2022). Confidence regions near singular information and boundary points with applications to mixed models. *The Annals of Statistics*, 50(3):1806–1832.
- Geyer, C. J. (1994). On the asymptotics of constrained M-estimation. *The Annals of Statistics*, 22(4):1993–2010.
- Guédon, T., Baey, C., and Kuhn, E. (2024). Bootstrap test procedure for variance components in nonlinear mixed effects models in the presence of nuisance parameters and a singular Fisher information matrix. *Biometrika*, page asae025.
- Harville, D. A. (1974). Bayesian inference for variance components using only error contrasts. *Biometrika*, 61(2):383–385.
- Jiang, W., Zhang, X., Li, S., Song, S., and Zhao, H. (2022). An unbiased kinship estimation method for genetic data analysis. *BMC bioinformatics*, 23(1):1–22.
- Kang, H. M., Sul, J. H., Service, S. K., Zaitlen, N. A., Kong, S.-y., Freimer, N. B., Sabatti, C., and Eskin, E. (2010). Variance component model to account for sample structure in genome-wide association studies. *Nature genetics*, 42(4):348–354.
- Kats, I., Vento-Tormo, R., and Stegle, O. (2021). Spatialde2: Fast and localized variance component analysis of spatial transcriptomics. *Biorxiv*, pages 2021–10.
- Lippert, C., Listgarten, J., Liu, Y., Kadie, C. M., Davidson, R. I., and Heckerman, D. (2011). Fast linear mixed models for genome-wide association studies. *Nature methods*, 8(10):833–835.
- Loh, P.-R., Tucker, G., Bulik-Sullivan, B. K., Vilhjalmsón, B. J., Finucane, H. K., Salem, R. M., Chasman, D. I., Ridker, P. M., Neale, B. M., and Berger, B. (2015). Efficient bayesian mixed-model analysis increases association power in large cohorts. *Nature genetics*, 47(3):284–290.
- Marx, V. (2021). Method of the year: spatially resolved transcriptomics. *Nature methods*, 18(1):9–14.
- Moore, R., Casale, F. P., Jan Bonder, M., Horta, D., Franke, L., Barroso, I., and Stegle, O. (2019). A linear mixed-model approach to study multivariate gene–environment interactions. *Nature genetics*, 51(1):180–186.

- Purcell, S. (2002). Variance components models for gene–environment interaction in twin analysis. *Twin Research and Human Genetics*, 5(6):554–571.
- Rotnitzky, A., Cox, D. R., Bottai, M., and Robins, J. (2000). Likelihood-based inference with singular information matrix. *Bernoulli*, 6(2):243–284.
- Schweiger, R., Fisher, E., Rahmani, E., Shenhav, L., Rosset, S., and Halperin, E. (2018). Using stochastic approximation techniques to efficiently construct confidence intervals for heritability. *Journal of Computational Biology*, 25(7):794–808.
- Schweiger, R., Kaufman, S., Laaksonen, R., Kleber, M. E., März, W., Eskin, E., Rosset, S., and Halperin, E. (2016). Fast and accurate construction of confidence intervals for heritability. *The American Journal of Human Genetics*, 98(6):1181–1192.
- Self, S. G. and Liang, K.-Y. (1987). Asymptotic properties of maximum likelihood estimators and likelihood ratio tests under nonstandard conditions. *Journal of the American Statistical Association*, 82(398):605–610.
- Stram, D. O. and Lee, J. W. (1994). Variance components testing in the longitudinal mixed effects model. *Biometrics*, 50(4):1171–1177.
- Stram, D. O. and Lee, J. W. (1995). Corrections: Variance component testing in the longitudinal mixed effects model. *Biometrics*, 51(3):1196.
- Svensson, V., Teichmann, S. A., and Stegle, O. (2018). SpatialDE: identification of spatially variable genes. *Nature methods*, 15(5):343–346.
- Visscher, P. M., Hill, W. G., and Wray, N. R. (2008). Heritability in the genomics era—concepts and misconceptions. *Nature reviews genetics*, 9(4):255–266.
- Weber, L. M., Saha, A., Datta, A., Hansen, K. D., and Hicks, S. C. (2022). nnsvg: scalable identification of spatially variable genes using nearest-neighbor gaussian processes. *bioRxiv*, pages 2022–05.
- Weissbrod, O., Geiger, D., and Rosset, S. (2016). Multikernel linear mixed models for complex phenotype prediction. *Genome research*, 26(7):969–979.
- Wood, S. N. (2013). A simple test for random effects in regression models. *Biometrika*, 100(4):1005–1010.

- Yang, J., Lee, S. H., Goddard, M. E., and Visscher, P. M. (2011). Gcta: a tool for genome-wide complex trait analysis. *The American Journal of Human Genetics*, 88(1):76–82.
- Zeng, Z., Li, Y., Li, Y., and Luo, Y. (2022). Statistical and machine learning methods for spatially resolved transcriptomics data analysis. *Genome biology*, 23(1):1–23.
- Zhang, Z., Ersoz, E., Lai, C.-Q., Todhunter, R. J., Tiwari, H. K., Gore, M. A., Bradbury, P. J., Yu, J., Arnett, D. K., Ordovas, J. M., et al. (2010). Mixed linear model approach adapted for genome-wide association studies. *Nature genetics*, 42(4):355–360.
- Zhou, X., Carbonetto, P., and Stephens, M. (2013). Polygenic modeling with Bayesian sparse linear mixed models. *PLoS genetics*, 9(2):e1003264.
- Zhou, X. and Stephens, M. (2012). Genome-wide efficient mixed-model analysis for association studies. *Nature genetics*, 44(7):821–824.